

# Bioavailability of mineral-associated trace metals as cofactors for nitrogen fixation by *Azotobacter vinelandii*

Shreya Srivastava<sup>1</sup> | Hailiang Dong<sup>1</sup>  | Oliver Baars<sup>2</sup> | Yizhi Sheng<sup>1</sup> 

<sup>1</sup>Department of Geology and Environmental Earth Science, Miami University, Oxford, Ohio, USA

<sup>2</sup>Department of Entomology and Plant Pathology, North Carolina State University, North Carolina, Raleigh, USA

## Correspondence

Hailiang Dong, Department of Geology and Environmental Earth Science, Miami University, Oxford, OH 45056, USA.  
Email: [dongh@miamioh.edu](mailto:dongh@miamioh.edu)

## Funding information

National Science Foundation, Grant/Award Number: EAR-1937423

## Abstract

Life on Earth depends on N<sub>2</sub>-fixing microbes to make ammonia from atmospheric N<sub>2</sub> gas by the nitrogenase enzyme. Most nitrogenases use Mo as a cofactor; however, V and Fe are also possible. N<sub>2</sub> fixation was once believed to have evolved during the Archean-Proterozoic times using Fe as a cofactor. However, δ<sup>15</sup>N values of paleo-ocean sediments suggest Mo and V cofactors despite their low concentrations in the paleo-oceans. This apparent paradox is based on an untested assumption that only soluble metals are bioavailable. In this study, laboratory experiments were performed to test the bioavailability of mineral-associated trace metals to a model N<sub>2</sub>-fixing bacterium *Azotobacter vinelandii*. N<sub>2</sub> fixation was observed when Mo in molybdenite, V in cavansite, and Fe in ferrihydrite were used as the sole sources of cofactors, but the rate of N<sub>2</sub> fixation was greatly reduced. A physical separation between minerals and cells further reduced the rate of N<sub>2</sub> fixation. Biochemical assays detected five siderophores, including aminochelin, azotochelin, azotobactin, protochelin, and vibrioferrin, as possible chelators to extract metals from minerals. The results of this study demonstrate that mineral-associated trace metals are bioavailable as cofactors of nitrogenases to support N<sub>2</sub> fixation in those environments that lack soluble trace metals and may offer a partial answer to the paradox.

## KEYWORDS

alternate nitrogenase, bioavailability, molybdenite, nitrogen fixation, nitrogenase

## 1 | INTRODUCTION

The geosphere and biosphere are linked through global biogeochemical cycles (Moore et al., 2017). All organisms require trace elements for growth and metabolism as they provide catalytic, electron transfer, and coordination properties to proteins (Zhang & Gladyshev, 2011). Most biologically important trace elements, such as Fe, Zn, Mo, Cu, Mn, Ni, and Co, are incorporated into certain proteins known as metalloproteins, which play important roles in various metabolic functions such as carbon, sulfur, and nitrogen metabolisms (Dupont et al., 2010). These trace elements are ultimately derived from minerals. The bioavailability of different trace metals depends on mineral solubility, which changes with mineral evolution through Earth history (Hazen et al., 2008). Bioavailability

of trace metals drives biological innovation of new metabolic pathways (Moore et al., 2017).

One particular nutrient, nitrogen (N), is essential for all life. However, bioavailable nitrogen is often the limiting nutrient for primary productivity as most organisms are unable to utilize N<sub>2</sub> in the atmosphere as the source of nitrogen (Bernhard, 2010). To be bioavailable, N<sub>2</sub> needs to be reduced to ammonia (NH<sub>3</sub>). In the modern world, biological reduction in N<sub>2</sub> to NH<sub>3</sub> is a major pathway of NH<sub>3</sub> formation (Ward, 2012). This process is known as diazotrophy or N<sub>2</sub> fixation and is carried out by nitrogenase enzymes. Biological N<sub>2</sub> fixation is energetically expensive (Dos Santos et al., 2004). Most nitrogenases use Mo as a metal cofactor, however, alternate cofactors such as V and Fe are also possible (Robson et al., 1986). Mo-based nitrogenase is the most common and efficient, because in oxic

environments, Mo is soluble and readily bioavailable (e.g.,  $\text{MoO}_4^{2-}$ ). Mo-nitrogenase has the highest catalytic activity (Eady, 1996). The Fe-only and V-based alternative nitrogenases are also important in natural environments, especially when Mo concentration is low (McRose et al., 2017). V-nitrogenase has been observed to increase  $\text{N}_2$  fixation rate in V-amended forest soils (Bellenger et al., 2014).

Alternative nitrogenases were once believed to have been important under the reducing conditions of early Earth, because of the low solubility of Mo-bearing minerals in anoxic oceans (Anbar & Knoll, 2002). Indeed, Mo isotope data from 3.0 Gyr iron formations suggest a low level of molybdate ions in seawater (Johnson et al., 2021). After the Great Oxidation Event (GOE), through oxidative weathering, Mo would have been mobilized from minerals and rocks as soluble  $\text{MoO}_4^{2-}$ , thus making the metal increasingly available for biological reactions (Jelen et al., 2016). Consistent with this scenario, Mo-based nitrogenase was once believed to have evolved after the GOE around 2.3–2.4 Gyr ago (Scott et al., 2008). However, new evidence argues for a Mo-dominant nitrogenase in the mid-Archaeon oceans, as early as 3.2 Gyr ago, even long before oxidative weathering became important. For example, tight distribution of nitrogen isotope fractionation of  $\sim 0\text{‰} \pm 1.5\text{‰}$  in sedimentary rocks (Stueken et al., 2015) supports the presence of such Mo-nitrogenase as early as the Mesoarchean age (3.2–2.8 Gyr). Furthermore, recent studies, employing phylogenetic analysis, ancestral sequence inference and structural homology modelling, suggest that Mo-based nitrogenase appears to be ancestral to the Fe or V versions (Boyd & Peters, 2013; Garcia et al., 2020; Parsons et al., 2021).

The emergence of the Mo-based nitrogenase Nif before the GOE raises an apparent paradox: dissolved Mo levels in the ocean were only a few nM (Johnson et al., 2021), yet geochemical and biological evidence suggests a widespread occurrence and function of Mo-based nitrogenase in Archaean oceans (Parsons et al., 2021). This apparent paradox is based on the untested assumption that only soluble Mo is bioavailable for use in Mo-based nitrogenase. Most studies investigating trace metal bioavailability consider soluble metals as the only bioavailable form, and there is little understanding of other sources of trace metals for various biogeochemical pathways including nitrogen fixation. We hypothesize that mineral-associated trace metals may be bioavailable and Mo-nitrogenase may have been synthesized on early Earth using mineral-associated Mo.

There are hints to support this hypothesis. In our previous study, Mo-based metabolic processes were detected in hot spring across temperature and pH gradients, even though soluble Mo was only measured at certain sites with circumneutral pH (Srivastava et al., 2018). This observation hints that there may be other sources of Mo. Furthermore, a previous study (Liermann et al., 2005) observed that a model  $\text{N}_2$ -fixing bacterium *Azotobacter vinelandii* was able to extract Mo from Fe- and Mo-enriched silicate glass for growth in the absence of soluble Mo. Apparently, *A. vinelandii* secreted a high-affinity ligand aminochelin (“molybdophore”) to extract Mo from the glass (Liermann et al., 2005). However, the authors neither used natural Mo- or Fe-containing minerals nor measured the rates of  $\text{N}_2$  fixation. Similarly, Knapp et al. (2007) demonstrated that the aerobic methanotroph *Methylosinus trichosporium* was able to extract Cu from Cu-doped iron

oxides and borosilicate glass. A fluorescent chromopeptide, called methanobactin, mediated the release of Cu from the solids and allowed the methanotroph to express pMMO gene, however, they did not measure the rates of methane oxidation (Knapp et al., 2007).

The objective of this study was to test the bioavailability of naturally occurring mineral-associated trace metals and their impact on  $\text{N}_2$  fixation rate, a first step toward understanding the ancestral origin of Mo-based nitrogenase. Experiments were performed where mineral-associated Mo, V, and Fe were used as the sole sources of trace metals for  $\text{N}_2$  fixation by *A. vinelandii*. Although the V and Fe bioavailability study does not directly address the origin of Mo-based nitrogenase, it would offer a meaningful comparison in testing bioavailability of different mineral-associated trace metals. The  $\text{N}_2$  fixation rate was measured using the acetylene reduction assay (ARA). Trace metal mobilization and siderophore production were analyzed, along with microscopic imaging of cell-mineral associations, to determine the potential microbial mechanisms of extracting these mineral-associated cofactors.

## 2 | MATERIALS AND METHODS

Two types of mineral-associated Mo, V, and Fe were prepared including adsorbed and structural forms. The reason for using these two types was to better understand the difference in bioavailability between sorbed and structurally bound metals. In the first type, metal cofactors were adsorbed onto minerals: (1) Mo sorption to ferrihydrite; (2) V sorption to goethite; (3) Fe sorption to montmorillonite. The use of ferrihydrite for Mo was because there is significant adsorption of molybdate on ferrihydrite at pH 6.8 (Gustafsson, 2003) and at pH 7.7 (Goldberg et al., 1996), the optimal growth pH range of *A. vinelandii*. Ferrihydrite is believed to have been formed during the Archaean through the photoferrotrophic oxidation of soluble Fe(II) in the marine photic zone (Konhauser et al., 2005). Goethite was used for V adsorption because similar to Mo, there is significant V adsorption to goethite at pH 6–8 (Peacock & Sherman, 2004). Goethite is also believed to have been present during the Archaean (Angerer & Hagemann, 2010). The reason for using montmorillonite for Fe sorption was because this clay mineral contains a minimal amount of Fe so that the bioavailability of sorbed Fe can be determined. Montmorillonite is the most common member of the smectite family. In addition to these sorbed forms, a second set of minerals included structurally bound metal cofactors. The minerals used for Mo, V, and Fe were molybdenite ( $\text{MoS}_2$ ), cavansite ( $\text{Ca}(\text{VO})\text{Si}_4\text{O}_{10}\cdot 4\text{H}_2\text{O}$ ), and ferrihydrite ( $\text{Fe}^{3+}_2\text{O}_3\cdot 0.5\text{H}_2\text{O}$ ), respectively. Molybdenite was available in the Archaean (Hazen et al., 2014). Cavansite was used as a model V-bearing mineral.

### 2.1 | Trace metal sorption

#### 2.1.1 | Ferrihydrite synthesis and Mo sorption

Ferrihydrite was synthesized by adapting the method from Schwertmann and Cornell (2007). Briefly, 50 mL of 0.06 M

$\text{FeCl}_3 \cdot 6\text{H}_2\text{O}$  was prepared in a 250 mL flask. The solution was vigorously stirred while 1 N NaOH was slowly added to raise the pH to 6.8. Molybdate was sorbed to freshly prepared ferrihydrite using a previous method (Gustafsson, 2003). Briefly, a stock solution of  $\text{Na}_2\text{MoO}_4$  (corresponding to  $50 \mu\text{M MoO}_4^{2-}$ ) was mixed with ferrihydrite suspension in 50 mL polypropylene centrifuge tubes in a solution of 0.01 M ionic strength (as  $\text{NaNO}_3$ ).  $\text{HNO}_3$  and NaOH were used to adjust the pH to circumneutral. After 24 h equilibrium, the sample was centrifuged for 10 min at 13,000g, and the pellet was collected and resuspended in an equal volume of Burk medium. This centrifugation–resuspension process was repeated three times to wash the Mo-ferrihydrite pellet and to eliminate any potential effect of  $\text{NaNO}_3$ . A previous study (Gustafsson, 2003) showed that at pH 6.8 most of the  $\text{MoO}_4^{2-}$  (~97%) should be sorbed to ferrihydrite. To confirm Mo sorption, the supernatants from all wash steps were analyzed by inductively coupled plasma-optical emission spectrometry (ICP-OES; Agilent Technologies) to measure the amount of remaining aqueous Mo concentration. The detection limit of the ICP-OES instrument was <0.6, <0.7 and <0.5 ng/mL for Fe, Mo, and V, respectively. The result confirmed nearly complete adsorption of Mo to ferrihydrite, equivalent to 9.6 mg Mo/g ferrihydrite (hereafter termed Mo-ferrihydrite).

### 2.1.2 | V sorption on goethite

A vanadium stock solution (100 ppm) was prepared by dissolving  $\text{V}_2\text{O}_5$  solid in deionized water. V was sorbed onto goethite (Sigma-Aldrich; Cat. # 71063) following a previous method (Peacock & Sherman, 2004). Briefly, 7.5 mL of the V stock solution of 25 ppm at pH 6 was added to 0.1 g goethite in 22.5 mL of 0.1 mM  $\text{NaNO}_3$  solution. The suspension was shaken continuously for 144 h followed by repeats of centrifugation and resuspension. The supernatants were analyzed with ICP-OES and the result showed 5.71 mg V/g goethite (hereafter termed V-goethite), which fell within the range of 4.9 mg/g (at pH 8) – 6.5 mg/g (at pH 6) reported by Peacock and Sherman (2004).

### 2.1.3 | Fe sorption to montmorillonite SWy-2

Sorption experiment was performed by mixing 100 mM aqueous  $\text{Fe}^{3+}$  ( $\text{FeCl}_3 \cdot 6\text{H}_2\text{O}$  in 0.1 N HCl) with a 10 g/L montmorillonite SWy-2 (hereafter referred to as SWy-2) suspension (Bhattacharyya & Gupta, 2008). SWy-2 was purchased from the Source Clays Repository of the Clay Minerals Society (Purdue University, IN). This mixture was shaken for a period of 10 h followed by three repeats of centrifugation and resuspension. The supernatants were analyzed using the 1,10-phenanthroline method (Amonette & Templeton, 1998) for dissolved Fe using a Genesys 10S UV-Vis spectrometer (Thermo Scientific). The result showed 0.56 mg Fe/g SWy-2 (hereafter termed Fe-SWy-2).

### 2.1.4 | Structurally bound trace metals

The trace metal containing minerals included molybdenite ( $\text{MoS}_2$ ), cavansite [ $\text{Ca}(\text{VO})\text{Si}_4\text{O}_{10} \cdot 4\text{H}_2\text{O}$ ], and ferrihydrite ( $\text{Fe}^{3+}_2\text{O}_3 \cdot 0.5 \text{H}_2\text{O}$ ). Molybdenite was acquired from the Limper Geology Museum of Miami University. Cavansite was purchased from an online source (Exquisite Crystals: <https://www.exquisitecrystals.com>). Ferrihydrite was synthesized as described above (Schwertmann & Cornell, 2007). Molybdenite was broken into small particles using a sterile scalpel and tweezers, while cavansite was broken using a mortar and pestle. The mineral particles were  $>10 \mu\text{m}$  as confirmed by SEM images.

### 2.1.5 | Strain and growth condition

*Azotobacter vinelandii* DJ (ATCC BAA-1303) was routinely cultured in a modified liquid Burk medium of the following composition:  $\text{KH}_2\text{PO}_4$ , 0.2 g;  $\text{K}_2\text{HPO}_4$ , 0.8 g;  $\text{MgSO}_4 \cdot 7\text{H}_2\text{O}$ , 0.2 g;  $\text{CaCl}_2 \cdot 2\text{H}_2\text{O}$ , 0.09 g; sucrose, 20 g at 30°C in a 150-rpm rotary shaker (Bishop et al., 1982). *A. vinelandii* was first revived in Burk medium with ammonium acetate ( $\text{NH}_4\text{OAc}$ ) as the nitrogen source. Subsequently, to promote diazotrophy, *A. vinelandii* was cultured in Burk medium with soluble Mo, V, and Fe but without  $\text{NH}_4\text{OAc}$ . To favor the use of Mo-dependent nitrogenase (Mo-diazotrophy),  $2 \mu\text{M Mo}$  (as  $\text{Na}_2\text{MoO}_4$ ) and  $52 \mu\text{M Fe}$  (as  $\text{FeSO}_4 \cdot 7\text{H}_2\text{O}$ ) were added to the Burk medium (hereafter termed Nif medium). In Nif medium, Fe was still required because it is part of the Mo- and V-dependent nitrogenases. This amount of Fe was considered replete (McRose et al., 2017). To favor V-diazotrophy (V-dependent nitrogenase),  $\text{V}_2\text{O}_5$  (final conc.  $100 \mu\text{M}$ ) was added to Burk medium along with  $52 \mu\text{M Fe}$  (Vnf medium). Anf medium (to favor Fe-dependent nitrogenase or Fe-diazotrophy) contained  $52 \mu\text{M Fe}$  only. *A. vinelandii* was cultured under each diazotrophy condition for 24–48 h at 30°C in a 150-rpm rotary shaker to achieve an  $\text{OD}_{620}$  of ~1 [ $\pm 0.16$ ]  $\times 10^8$  cells/mL (Wichard et al., 2009). After cell growth, the suspension was centrifuged for 10 min at 6000g, and the pellet was collected and resuspended in an equal volume of Burk medium but without any trace metals. This centrifugation–resuspension process was repeated three times to eliminate any carryover of aqueous metals from initial growth. This inoculum was used to determine the ability of mineral-associated trace metals as cofactors for nitrogenase activity under the respective diazotrophic condition.

### 2.1.6 | $\text{N}_2$ -fixation rate measurement

To test the bioavailability of solid source trace metals, Mo-ferrihydrite or molybdenite replaced aqueous Mo (up to  $2 \mu\text{M}$  aqueous concentration assuming full dissolution) in Nif medium, V-goethite or cavansite replaced aqueous V (up to  $150 \mu\text{M}$ ) in Vnf medium, and Fe-SWy-2 or ferrihydrite replaced aqueous Fe (up to  $52 \mu\text{M}$ ) in Anf medium. The corresponding mass concentrations of Mo-ferrihydrite, V-goethite, and Fe-SWy-2 were 0.02, 1.35, and 5.20 g/L, respectively, while those of

molybdenite, cavansite, and ferrihydrite were 0.32, 67, and 9 mg/L, respectively. The 30-mL serum vials contained 10 mL medium and were sealed using butyl rubber septa. The medium and the headspace were each purged with He for 30 min, followed by sterilization at a temperature of 121°C and a pressure of 103 kPa for 30 min. Finally, 1 mL of *A. vinelandii* inoculum ( $OD_{620}$  of ~1) grown in the corresponding aqueous metal medium was added with a syringe needle to achieve a final  $OD_{620}$  of ~0.1. Positive controls contained aqueous forms of Mo, V, and Fe (i.e., Nif, Vnf and Anf medium, respectively). In an abiotic control, 1 mL cell suspension was replaced by the same amount of Burk medium. All experiments were conducted in triplicates.

The bioavailability of mineral-associated metals was assessed by measuring the rate of  $N_2$  fixation with the Acetylene Reduction Assay (ARA). The ARA is widely used to measure the rate of  $N_2$ -fixation because nitrogenases are able to similarly reduce acetylene to ethylene ( $C_2H_4$ ) and  $N_2$  to ammonia (Dilworth, 1966). We assume that ARA is similarly effective for measuring the rate of  $N_2$  fixation using nitrogenases synthesized from both forms of trace metals (adsorbed and structurally bound). The assay was initiated by injecting 2 mL of high purity (99.6%) (Airgas) acetylene into the headspace of the serum vials after removing 2 mL He (i.e., ~10% acetylene and ~90% helium in the headspace). The amount of ethylene produced from acetylene reduction was determined in a 250  $\mu$ L subsample of the headspace. Subsamples were collected every 15 min using a gas-tight syringe. The syringe was flushed for four times with He gas. The ARA was conducted for a period of 4 h, because a longer time would exhaust dissolved  $O_2$  in the medium and inactivate *A. vinelandii* cells. Ethylene concentration in the subsamples was measured using gas chromatography (Varian 3300 Gas Chromatography) equipped with an 80/100 Porapak Q column and flame ionization detector using nitrogen as the carrier gas. The temperature of the injector and detector was maintained at 100°C and the column at 50°C. Ethylene concentration was determined by comparing to a freshly prepared standard using ultra high purity ethylene gas (99.9%) (Airgas). A calibration curve was pre-established relating the peak area to ethylene (nmol) amount. Ethylene amount at the end of 4 h was calculated as follows:

$$\text{Ethylene amount} = [(E_{\text{total}})_f - (E_{\text{total}})_0],$$

where ethylene amount ( $E_{\text{total}}$ ) = (nmol  $C_2H_4$ /mL)  $\times$   $V_{\text{headspace}}$ .

$$V_{\text{headspace}} = V_{\text{total}} - V_{\text{water}}.$$

The rate of nitrogen fixation was calculated as follows:

$$\text{Rate} = [(E_{\text{total}})_f - (E_{\text{total}})_0] / (\Delta t),$$

$$\Delta t = t_f \text{ (final time point)} - t_0 \text{ (initial time point)}.$$

### 2.1.7 | Trace metal measurements

In the  $N_2$ -fixation rate measurement, Burk medium itself may have contained some trace metals that would affect  $N_2$  fixation. In

addition, Nif, Vnf, and Anf media may leach mineral-associated trace metals without the action of *A. vinelandii* cells. Therefore, three experiments were conducted to measure: (1) the background amounts of Mo, V and Fe in Burk medium; (2) the amounts of passive Mo release from Mo-ferrihydrite and molybdenite in Nif medium (i.e., in the presence of 52  $\mu$ M aqueous Fe), V release from V-goethite or cavansite in Vnf medium (i.e., in the presence of 52  $\mu$ M aqueous Fe), and Fe release from Fe-SWy-2 or ferrihydrite in Anf medium (i.e., no aqueous Fe); (3) Dissolved concentrations of Fe, Mo, and V in the presence of *A. vinelandii* cells. After a period of either 24 (for metal desorption from Mo-ferrihydrite, V-goethite, and Fe-SWy-2) or 72 h (for metal release from abiotic dissolution of molybdenite, cavansite or ferrihydrite), supernatant samples were collected by centrifugation at 8000g for 10 min followed by syringe filtration (0.22  $\mu$ m polypropylene sterile syringe filter) (ThermoFisher). The samples were acidified (2% v/v  $HNO_3$ ) and analyzed by ICP-OES. To confirm if any trace metals passively released from abiotic desorption or mineral dissolution were sufficient to fix  $N_2$ , aliquots of the above supernatant solutions were used for  $N_2$  fixation rate measurements.

### 2.1.8 | Dialysis bag experiments

To test whether *A. vinelandii* required a direct contact to produce siderophores and other metabolites as a mechanism of extracting mineral-associated trace metals (Ahmed & Holmstrom, 2015), the minerals were placed inside a dialysis bag (~0.01  $\mu$ m pore size, molecular weight cut-off (MWCO) 12,000–14,000 Da; ThermoFisher), while *A. vinelandii* cells were in bulk solution. This pore size of the bag would not allow passage of any cells or mineral particles but should not hinder passage of secondary metabolites with a molecular weight <1500 Da (Rai et al., 2020).

### 2.1.9 | Pre-acclimation experiment

Molybdenite, cavansite, and ferrihydrite may not be readily available to support  $N_2$  fixation, likely due to their crystalline structures. Thus, in certain experiments, *A. vinelandii* cells were pre-acclimated to these minerals for 24–96 h as the sole sources of Mo, V, and Fe in Nif, Vnf, and Anf media, respectively, followed by ARA experiments. Because wild-type *A. vinelandii* has a generation time of 4 h under diazotrophic condition, the incubation period of 24–96 h would constitute at least 6–24 generations (Mus et al., 2017).

### 2.1.10 | Siderophore quantification

*Azotobacter vinelandii* is known to produce siderophores as a strategy to increase the bioavailability of mineral-associated trace metals (Liermann et al., 2005). To quantify various siderophore production in response to Mo-, V-, and Fe-diazotrophy, *A. vinelandii* was

incubated in separate experiments. Different from the ARA measurement (4 h culture starting with an OD of 0.1), in this experiment a lower inoculum (OD ~0.005) was used and siderophore production was analyzed during exponential and early stationary phases after 24 and 48 h incubation, respectively (final ODs = 1.1–1.7). The longer incubation time and higher biological growth usually lead to more siderophore production. Siderophore samples were syringe filtered (0.22  $\mu\text{m}$ ) and analyzed with LC-MS (Ultimate 3000 UPLC/ISQ EC; Thermo Fisher Scientific) as described previously (Baars et al., 2016). The final siderophore concentrations were normalized to the optical density (OD) of *A. vinelandii*.

### 2.1.11 | Microscopic observations of mineral-microbe association

Scanning electron microscopy (SEM) was performed for some selective experimental groups to visualize cell-mineral associations. *A. vinelandii* was grown for 48 h in Nif and Vnf media with molybdenite and cavansite as the sole sources of Mo and V, respectively. Subsequently, cell-mineral suspensions were fixed using 2.5% glutaraldehyde and 2% paraformaldehyde in 0.05 M sodium cacodylate buffer followed by stepwise dehydration in increasing concentrations of ethanol (25%, 50%, 75%, 95%, and 100%) and critical point drying (CPD) (Dong et al., 2003). Finally, the samples were mounted on SEM stubs and sputter-coated with gold before imaging using a Zeiss Supra 35 VP Field Emission Scanning Electron Microscope with an accelerating voltage of 7 kV and a working distance of 9.5 mm.

## 3 | RESULTS

### 3.1 | Microbial release of mineral-associated trace metals

The background levels of Mo and V in Burk medium were found to be below detection limit (BDL) of the ICP-OES method (Table S1). However, there was a small amount of background Fe in Burk medium (4.04  $\mu\text{M}$ ). In the absence of bacteria, the amount of desorption of Mo from Mo-ferrihydrite, V from V-goethite, and Fe from Fe-SWy-2 was 0.02, 0.37, and 0.70  $\mu\text{M}$ , respectively. There were certain levels of aqueous Fe because the desorption experiments were conducted in Nif, Vnf, and Anf media, where 52  $\mu\text{M}$  aqueous Fe was added except the case of Fe-SWy-2. However, the measured Fe concentrations in Mo-ferrihydrite (in Nif medium) and V-goethite (in Vnf medium) were lower than 52  $\mu\text{M}$ , likely because of adsorption. Without bacteria, aqueous Mo from dissolution of molybdenite, V from cavansite, and Fe from ferrihydrite in their respective medium (Nif, Vnf, and Anf, respectively) were all BDL (Table S1). Apparently, molybdenite and cavansite did not sorb any added aqueous Fe, and ferrihydrite did not release any Fe from its structure. pH decreased slightly from ~7.2 to ~6.9 during all these abiotic experiments.

In the presence of *A. vinelandii* cells, positive controls (with aqueous trace metals) showed time-course consumption. In particular, aqueous Mo and Fe concentrations decreased from 2.05 to 0.39  $\mu\text{M}$  and from 52.99 to 1.08  $\mu\text{M}$ , respectively (Table 1). However, in V-diazotrophy, it was the aqueous Fe, not the V, that was actually consumed. When both *A. vinelandii* cells and minerals were present, aqueous concentrations of metals all increased. For example, Mo release from molybdenite was BDL in abiotic control (Table S1), but after 24-h incubation with *A. vinelandii*, it increased to 0.35  $\mu\text{M}$  (Table 1). Likewise, the amount of aqueous V released from V-goethite increased from 0.37  $\mu\text{M}$  due to abiotic desorption to 2.61  $\mu\text{M}$  in biotic treatment. The amount of aqueous V from cavansite dissolution increased from BDL in abiotic control to 2.25  $\mu\text{M}$  in the presence of microbial activity. A similar case was observed for ferrihydrite. pH decreased slightly from ~7.3 to ~6.9 in all biotic experiments.

**TABLE 1** Aqueous trace metal concentrations in the supernatant of the three diazotrophy conditions.

Sample name	Fe ( $\mu\text{M}$ )	Mo ( $\mu\text{M}$ )	V ( $\mu\text{M}$ )
Aq. Mo 0	52.99	2.05	BDL
Aq. Mo 24	1.08	0.39	0.13
Mo-ferrihydrite 0	53.56	BDL	BDL
Mo-ferrihydrite 24	0.53	BDL	BDL
Mo-ferrihydrite DB 0	53.40	BDL	BDL
Mo-ferrihydrite DB 24	BDL	BDL	BDL
Molybdenite 0	53.24	BDL	BDL
Molybdenite 24	62.54	0.35	BDL
Aq. V 0	52.33	0.02	132.88
Aq. V 24	0.62	BDL	156.62
V-goethite 0	52.06	BDL	BDL
V-goethite 24	1.03	BDL	2.61
V-goethite DB 0	51.76	BDL	BDL
V-goethite DB 24	0.28	BDL	2.03
Cavansite 0	53.56	BDL	BDL
Cavansite 24	1.18	BDL	2.25
Aq. Fe 0	52.17	0.01	BDL
Aq. Fe 24h	1.40	BDL	BDL
Fe-Swy2 0	BDL	BDL	BDL
Fe-Swy2 24h	0.77	BDL	BDL
Fe-Swy2 DB 0	BDL	BDL	BDL
Fe-Swy2 DB 24	0.56	BDL	BDL
Ferrihydrite 0	BDL	BDL	BDL
Ferrihydrite 24	0.53	BDL	0.02

Note: Error (+/-): <2%. Abbreviations for the different sources follow Figures 1–3. Abbreviations for sampling times are: T0 (0 h) and T24 (24 h). The total concentrations of Mo, V and Fe (either in aqueous or sorbed form) are 2  $\mu\text{M}$  Mo, 150  $\mu\text{M}$  V, and 52  $\mu\text{M}$  Fe, respectively. Starting aqueous concentration of  $\text{Fe}^{2+}$  in Mo- and V-diazotrophic conditions was 52  $\mu\text{M}$  (in the form of  $\text{FeSO}_4$ ).

Abbreviation: BDL, below detection limit.

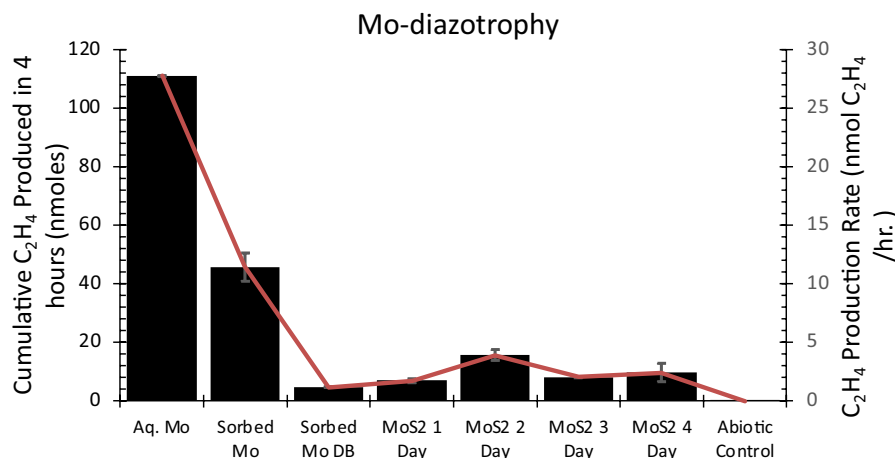


**FIGURE 1** Amount of ethylene produced by the end of 4 h (1st y-axis) and the average ethylene production rate (2nd y-axis) under Mo-diazotrophy conditions. The relative amount of nitrogen fixation with aq. Mo was taken as 100% for the purpose of comparison with other Mo sources. Abbreviations for the different sources are aqueous Mo (Aq. Mo), Mo-Fh (Mo-ferrihydrite), Mo-Fh DB (Mo-ferrihydrite in dialysis bag), Moly. 24, 48, 72, and 96 h (molybdenite with pre-incubated inoculum for 24, 48, 72, and 96 h).

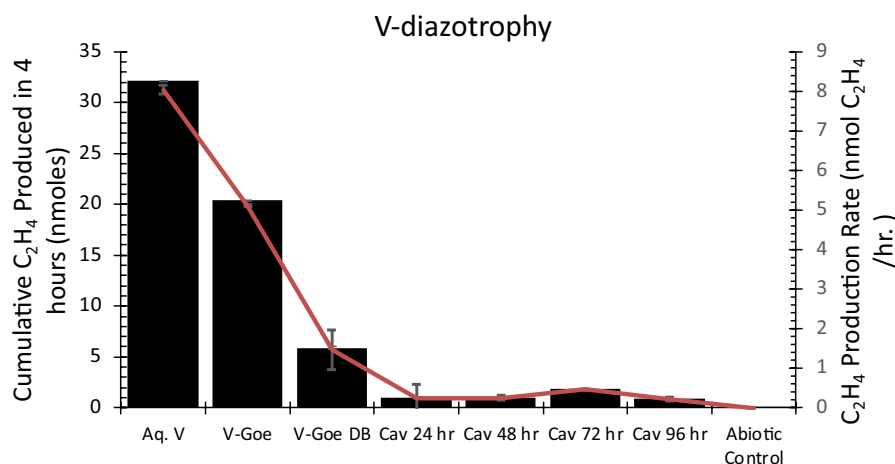


**FIGURE 2** Amount of ethylene produced by the end of 4 h (1st y-axis) and the average ethylene production rate (2nd y-axis) under V-diazotrophy condition. The relative amount of nitrogen fixation with aq. V was taken as 100% for the purpose of comparison with other V sources. Abbreviations for different sources of V are aqueous V (Aq. V), V-Goe (V-Goethite), V-Goe DB (V-goethite in dialysis bag), Cav 24, 48, 72, and 96 h (cavansite with pre-incubated inoculum for 24, 48, 72, and 96 h).

### 3.2 | N<sub>2</sub> fixation rate

#### 3.2.1 | N<sub>2</sub> fixation rate with mineral sorbed-trace metals

The N<sub>2</sub> fixation rate is usually normalized to biomass (Bellenger et al., 2011), however, over the short measurement duration used in this study (4 h), biomass did not change (OD<sub>620</sub> within the range of 0.10–0.11). Therefore, the N<sub>2</sub> fixation rate was expressed as both cumulative ethylene production over 4 h (nmol) and ethylene production rate (nmol/h).

As expected, *A. vinelandii* was able to use aqueous forms of Mo, V, and Fe for N<sub>2</sub> fixation. Relative to aqueous Mo, the ethylene production rate with aqueous V and Fe was 71% and 76% lower, respectively (Figure S1). Using abiotic leachates in the Nif, Vnf, and Anf media, neither the total amount nor the

rate of ethylene production was higher than that in the presence of 52 μM aqueous Fe alone, suggesting that any aqueous Mo, V, and Fe passively released from the minerals were not sufficient to stimulate N<sub>2</sub> fixation. Interestingly, *A. vinelandii* utilized mineral-adsorbed trace metals for N<sub>2</sub> fixation but with reduced rates. By the end of 4 h and with an inoculum OD<sub>620</sub> of ~0.1, the average rate of ethylene production was 28 nmol/h. When aqueous Mo was used, with a total of 111 nmol of ethylene production (Figure 1). However, when Mo-sorbed ferrihydrite was used, the average rate was only 11 nmol/h, 59% lower than that when aqueous Mo was used, with a total of 46 nmol of ethylene produced. Similarly, the average rates of ethylene production with V-sorbed goethite and Fe-sorbed SWy-2 were 5 and 4 nmol/h, respectively, which was 37% and 42% lower than their aqueous equivalents (Figures 2 and 3). Likewise, the amounts of ethylene production with V-sorbed goethite and Fe-sorbed SWy-2 were

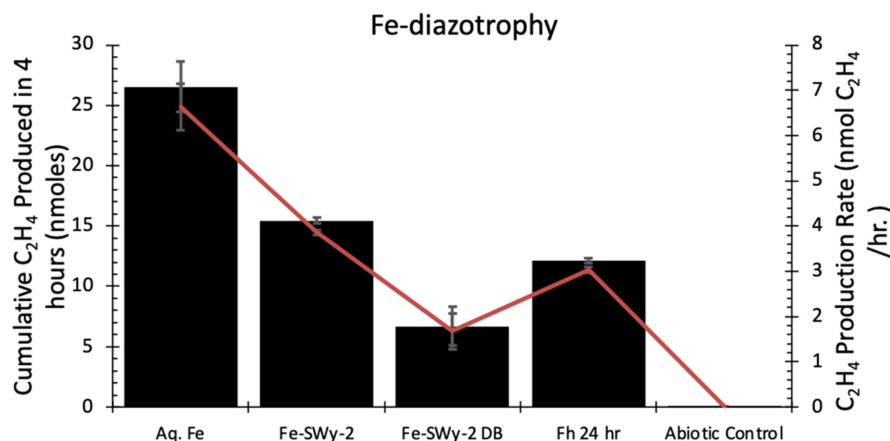


**FIGURE 3** Amount of ethylene produced by the end of 4 h (1st y-axis) and the average ethylene production rate (2nd y-axis) under Fe-diazotrophy condition. The relative amount of nitrogen fixation with aq. Fe was taken as 100% for the purpose of comparison with other Fe sources. Abbreviations for the different sources are aqueous Fe (Aq. Fe), Fe-SWy-2 (Fe-Montmorillonite SWy-2), Fe-SWy-2 DB (Fe-Montmorillonite SWy-2 in dialysis bag) and ferrihydrite (Fh).

32 and 15 nmol, respectively (Figures 2 and 3). The average rate of ethylene production with Mo-ferrihydrite (11 nmol/h) was higher than that with aqueous Fe (7 nmol/h). The total amount of ethylene production by the end of 4 h with Mo-ferrihydrite (46 nmol) was also higher than that with aqueous Fe (27 nmol), even when both were present in the Nif medium, suggesting that adsorbed Mo (Mo-ferrihydrite) was a preferred metal cofactor over aqueous Fe.

### 3.2.2 | Nitrogen fixation with structurally bound trace metals

When *A. vinelandii* inoculum was incubated with molybdenite and cavansite as the sole sources for Mo- and V-diazotrophy, respectively, a negligible amount of ethylene was produced after 4 h (data not shown). Therefore, a pre-acclimated culture was used to measure the N<sub>2</sub> fixation rate. The average rate of ethylene production by the inoculum that was pre-acclimated with molybdenite for 24 h was 2 nmol/h (Figure 1) with a total of 7 nmol of ethylene produced (Figure 1). The rate and total amount of ethylene production doubled when the pre-acclimation time increased to 48 h. However, a further increase in pre-acclimation time decreased the rate of ethylene production, possibly due to over-growth of culture, decrease of nutrient supply, and accumulation of toxic waste products (Mukhtar et al., 2018). When compared with aqueous Mo, even with the optimal pre-acclimation time (48 h), the rate of ethylene production with molybdenite was still 86% lower, with a total of 16 nmol of ethylene produced (Figure 1). Similarly, in case of cavansite, the average rate of ethylene production with pre-acclimated inoculum for 24–72 h was 0.2–0.5 nmol/h (Figure 2) with only 1–2 nmol of ethylene produced (Figure 2). When compared to aqueous V, even with the optimal pre-incubation time (72 h), the rate of ethylene production with cavansite was 94% lower with a total of only 2 nmol of ethylene produced (Figure 2).

Ferrihydrite was a better source of Fe for Fe-diazotrophy compared with molybdenite and cavansite for Mo- and V-diazotrophy, respectively, because the average rate of ethylene produced was only 54% lower than that with aqueous Fe. After 4 h, the average rate of ethylene production using inoculum that was pre-acclimated with ferrihydrite for 24 h was 3 nmol/h (Figure 3), with a total of 12 nmol of ethylene production (Figure 3). These results indicate that of the three structural trace metal sources tested, ferrihydrite was the most effective for Fe-diazotrophy by *A. vinelandii*, consistent with more bioavailable nature of ferrihydrite.

### 3.2.3 | Effect of dialysis bag on the N<sub>2</sub> fixation rate

When Mo-ferrihydrite, V-goethite, and Fe-SWy-2 were enclosed inside a dialysis bag, the average ethylene production rate was only 1 nmol/h with Mo-ferrihydrite (Figure 1a), 1 nmol/h with V-goethite (Figure 2), and 2 nmol/h with Fe-SWy-2 (Figure 3). These rates were 96%, 82%, and 75% lower than their aqueous equivalents. The total amount of ethylene production was 6, 5 and 7 nmol for these three treatments, respectively (Figures 1–3), again significantly lower than their aqueous equivalents.

### 3.2.4 | Siderophore analysis

*Azotobacter vinelandii* produces three classes of siderophores: the weak  $\alpha$ -hydroxycarboxylate siderophore vibrioferrin, catechol siderophores (2,3-dihydroxybenzoic acid, aminochelin, azotochelin, protochelin), and azotobactins (Baars et al., 2016). Among these, aminochelin (Liermann et al., 2005) and azotochelin (Duhme et al., 1998) are known to bind Mo. These siderophores were quantified in all experimental incubations (Table S2). Unexpectedly, there was no significant correlation between Fe availability and production of siderophores. The highest

siderophore concentrations were detected in Mo-diazotrophy (Figure 4), followed by V- (Figure 5) and Fe-diazotrophy (Figure 6). Interestingly, the highest siderophore concentrations were produced in cultures where cofactors were supplied in the forms of minerals. By contrast, siderophore concentrations were much lower with aqueous metals or when the minerals were enclosed inside a dialysis bag. Generally, the siderophore pool consisted of vibrioferrin, aminochelin and azotochelin, while azotobactin and protochelin were negligible.

The highest siderophore production was detected in the 24 h molybdenite culture (Figure 4), with a dominant amount of vibrioferrin (up to  $\sim 178 \mu\text{M}$  per OD), and smaller amounts of aminochelin and azotochelin ( $\sim 35 \mu\text{M}$  each). This condition had the highest dissolved Fe concentration, suggesting that siderophore production may have been induced by factors other than a low level of dissolved iron. The second highest vibrioferrin production was observed in Mo-sorbed ferrihydrite culture ( $\sim 105 \mu\text{M}$ ). However, when Mo-sorbed ferrihydrite was supplied in a dialysis bag, only small amounts of siderophores were detected (up to  $2 \mu\text{M}$ ), although cells reached similar optical densities. These data suggest that a physical contact between cells and mineral surface may be required to enhance the production of siderophores.

### 3.2.5 | Microscopic mineral-microbe associations

Spherical *A. vinelandii* cells attached to molybdenite (Figure 7) and cavansite (Figure 8) surfaces when these minerals served as the sole sources of Mo and V in the medium. These images were consistent with increased aqueous concentrations of Mo and V after 24 h of incubation (Table 1), suggesting that *A. vinelandii* were able to extract these trace metals from minerals by physical attachment.

## 4 | DISCUSSION

### 4.1 | Biological $\text{N}_2$ fixation using mineral-associated trace metals

Because aqueous Fe ( $\sim 52 \mu\text{M}$ ) was added to Nif and Vnf media in the presence of mineral-associated Mo and V, there may be ambiguity of the actual metals used for  $\text{N}_2$  fixation (aqueous Fe or mineral-associated Mo, V, or Fe). However, multiple lines of evidence strongly suggest that mineral-associated Mo, V, or Fe were bioavailable, in addition to or as alternative to aqueous Fe.

First, the average ethylene production rate with aqueous Fe ( $< 7 \text{ nmol/h}$ ) was much lower than that with Mo-ferrihydrite ( $11 \text{ nmol/h}$ ). Likewise, the total amount of ethylene produced after 4 h with aqueous Fe ( $27 \text{ nmol}$ ) was much lower than that with Mo-ferrihydrite ( $46 \text{ nmol}$ ). These results suggest that at least some sorbed Mo was utilized for nitrogenase synthesis. It was likely that both Fe- and Mo-nitrogenases may have been responsible for the amount of ethylene production. In either case, Mo-nitrogenase should have contributed to  $\text{N}_2$  fixation.

Second, in case of molybdenite, the average rate and amount of ethylene production were much lower ( $2\text{--}4 \text{ nmol/h}$  and a total of  $7\text{--}16 \text{ nmol}$ , respectively) than that with aqueous Fe alone ( $7 \text{ nmol/h}$  and a total of  $27 \text{ nmol}$ , respectively). Aqueous Fe did not appear to sorb to molybdenite surface (Table S1). Furthermore, unlike aqueous Fe-diazotrophy where its concentration was consumed after 24 h, its concentration in the molybdenite experiment actually significantly increased (Table 1). The only explanation was the use of a Mo-based nitrogenase for the observed  $\text{N}_2$ -fixation activity, even in the presence of ample aqueous Fe (Table S1). The source of aqueous Mo likely came from active extraction of Mo from molybdenite by *A. vinelandii* cells ( $0.35 \mu\text{M}$  in the presence of bacteria versus BDL in

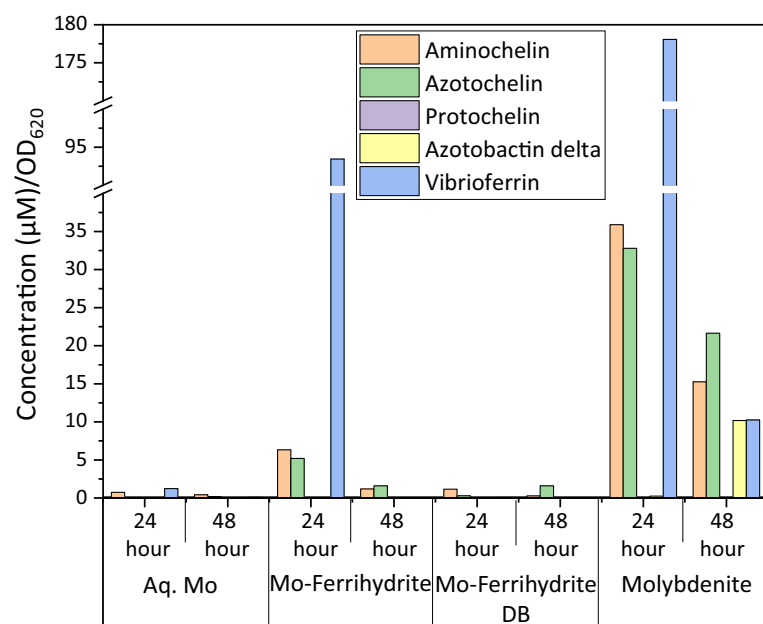
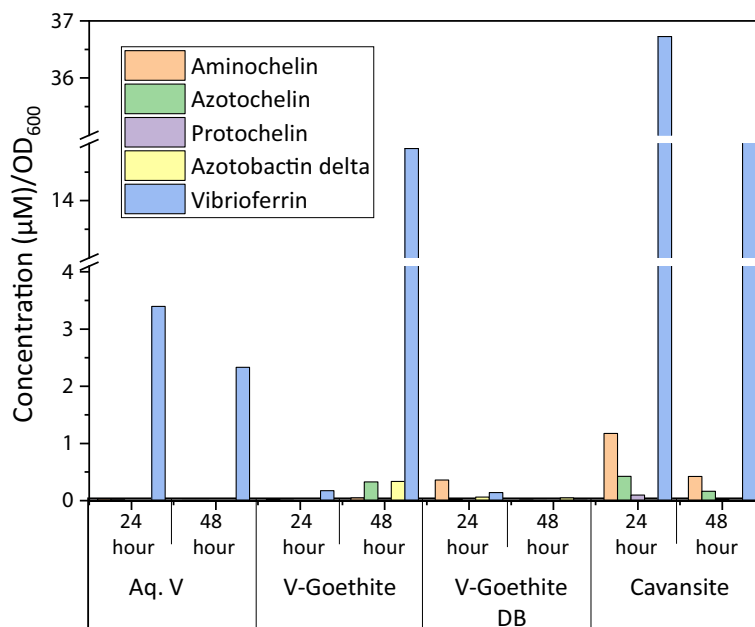
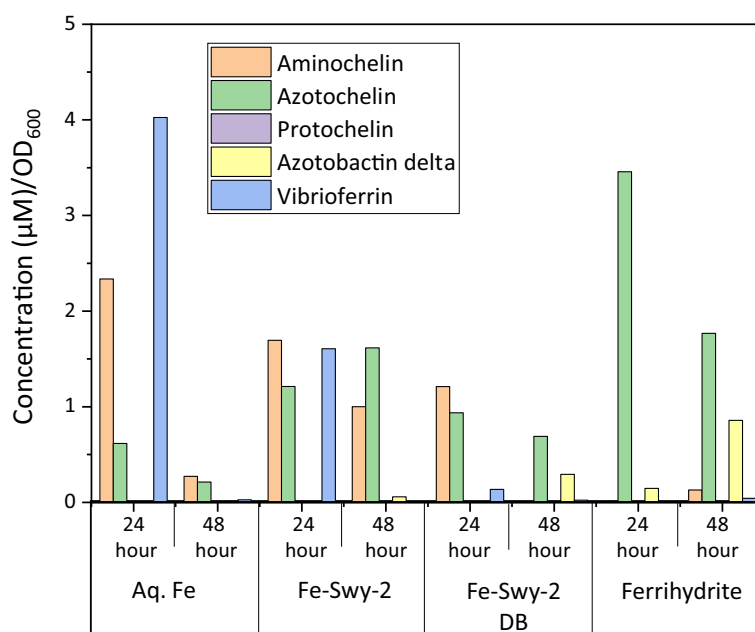


FIGURE 4 Siderophore production under Mo-diazotrophy condition using different sources of Mo at 24 and 48 h. Abbreviations for the sources follow Figure 1.

**FIGURE 5** Siderophore production under V-diazotrophy condition using different sources of V at 24 and 48 h. Abbreviations for the different sources follow [Figure 2](#).



**FIGURE 6** Siderophore production under Fe-diazotrophy condition using different sources of Fe at 24 and 48 h. Abbreviations for the different sources follow [Figure 3](#).



their absence) ([Table 1](#); [Table S1](#)). Molybdenite may have also contained some Fe and released it to solution upon biotic dissolution, thus accounting for its concentration increase after 24 h.

Third, a previous study showed that *A. vinelandii* produces a high-affinity ligand ("molybdophore"), aminochelin, to extract Mo from a silicate glass under Mo-limited and Fe-replete conditions (Liermann et al., 2005). Our data are consistent showing higher amounts of aminochelin in the presence of Mo-ferrhydrite and molybdenite than in the presence of aqueous Mo and ferrhydrite ([Figures 4 and 6](#)).

A similar case was observed for V-diazotrophy. The average rates and amounts of ethylene production were much lower with mineral-associated V (5 nmol/h and a total of 20 nmol with V-goethite, and <1 nmol/h and a total of 1–2 nmol for cavansite) than that with

aqueous Fe (7 nmol/h and a total of 27 nmol), even in the presence of added aqueous Fe ([Table S1](#)). A higher concentration of vibrioferriin was detected in the presence of these V minerals ([Figure 5](#)) than under any Fe-diazotrophy condition ([Figure 6](#)). High production of vibrioferriin has been previously observed under conditions of "mild" Fe limitation (Baars et al., 2016; Zhang et al., 2019), but its role in V complexation is unclear. Nonetheless, it cannot be ruled out that *A. vinelandii* might have employed vibrioferriin to obtain V from minerals. Indeed, aqueous V concentration significantly increased from 0.37 to 2.61  $\mu\text{M}$  in the V-goethite treatment and from BDL to 2.25  $\mu\text{M}$  in the cavansite treatment ([Table 1](#); [Table S1](#)), most likely due to active extraction of V from these minerals by *A. vinelandii* cells.

These results collectively suggested that vibrioferrin, along with aminochelin and azotochelin, may be involved in active microbial extraction of Mo and V from minerals. This suggests that if potential solid-phase Mo and V sources are available, *A. vinelandii* preferentially expresses *nif* and *vnf* over *anf* genes even under conditions of depleted aqueous Mo and V but excess aqueous Fe. Further work is necessary to better explain these observations.

Suppressed production of siderophores in the presence of a dialysis bag suggests that a physical contact was necessary for their production. Previous studies have observed enhanced siderophore production upon microbial attachment to silicate mineral surface (Ahmed & Holmstrom, 2015). A possible mechanism is facilitated formation of metal-siderophore complex at the mineral surface (Ahmed & Holmstrom, 2015). Once produced, these siderophores were likely responsible for extraction of metals from minerals, as

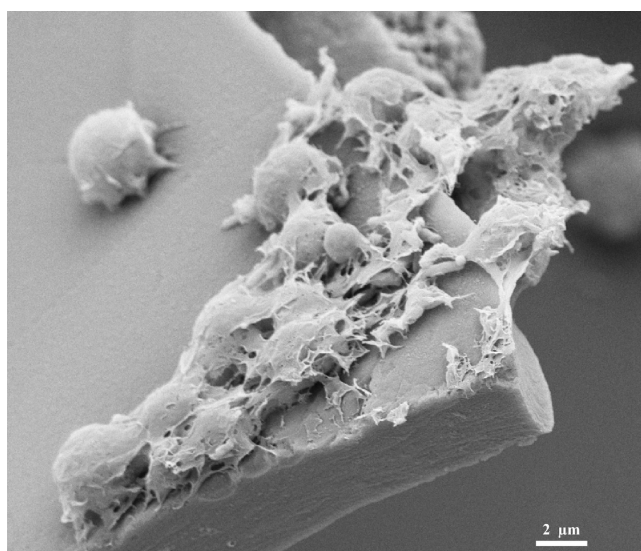


FIGURE 7 SEM micrograph depicting *Azotobacter vinelandii* cell attachment on molybdenite surface.

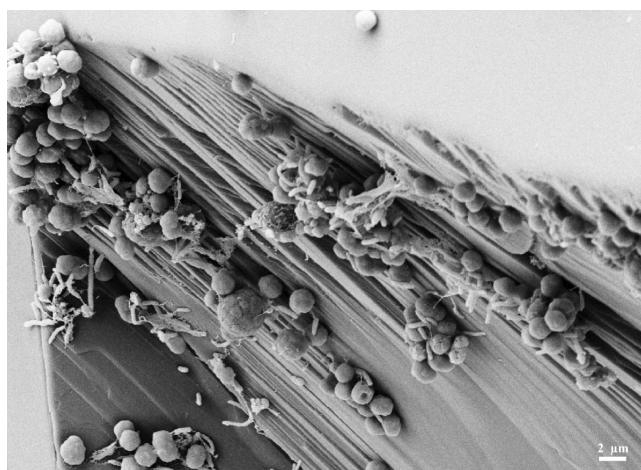


FIGURE 8 SEM micrograph depicting *Azotobacter vinelandii* cell attachment on cavansite surface.

observed in this study. Although pH was previously considered an important factor in microbial extraction of Ni from silicate glass by a methanogen (Hausrath et al., 2007), it was not likely responsible for enhanced metal release in this study because the change in pH was similar between abiotic control and biotic experiments (both within 0.3 units).

## 4.2 | Bioavailability of mineral-associated trace metals on modern Earth

A common assumption in microbial ecology is that only soluble trace metals are bioavailable to support microbial growth and functions. However, this assumption often has difficulty in explaining field observations. For example, Warren et al. (2017) discovered that Mo-nitrogenase dominated over Fe- and V-nitrogenases, despite lower concentrations of dissolved Mo (1–7 nM) than dissolved V (5–21 nM) and dissolved Fe (7–35 nM). Our previous work (Srivastava et al., 2018) observed that despite undetectable levels of soluble Mo in many Tengchong hot springs, processes and organisms that require Mo were actually detected and even abundant. These results could have been better reconciled if solid-source Mo was considered. Indeed, Liermann et al. (2005) demonstrated that trace metals in Fe- and Mo-enriched silicate glass were bioavailable to the model  $N_2$ -fixing bacterium *A. vinelandii*. This organism secreted siderophores to extract Mo from silicate glass. In fact, bioavailability of solid-state trace metals is not limited to Mo. For example, the methanotroph, *M. trichosporium* OB3b, was able to acquire Cu from iron oxides and silicate glass (Knapp et al., 2007; Kulczykcki et al., 2011) and this ability influenced  $CH_4$  oxidation rate. *M. trichosporium* OB3b produced a Cu-binding ligand methanobactin to enhance Cu dissolution (Chi Fru et al., 2011). However, Warren et al. (2017) and Srivastava et al. (2018) did not measure bioavailability of solid-form Mo, while Liermann et al. (2005) did not measure  $N_2$ -fixation rate.

By directly testing the bioavailability of trace metals in naturally occurring minerals and their impact on  $N_2$  fixation rate, this study potentially links laboratory mechanistic investigation to field observation. We demonstrated that mineral-associated trace metals are bioavailable to support  $N_2$  fixation. Low rates of  $N_2$  fixation can be compensated by extended time in natural ecosystems. Furthermore, dynamic natural systems can remove the product (ammonium) and expose new mineral surface, thus possibly sustaining the reaction over time. Siderophores may be secreted by  $N_2$ -fixing microorganisms themselves or by other organisms and even plants to help microbial acquisition of trace metals from minerals (Kraemer et al., 2019). The results of this study are particularly relevant to life on land, because unlike the oceans where there are certain levels of dissolved Mo [a few nM in Archean oceans (Johnson et al., 2021) and ~107 nM in modern oceans (Collier, 1985)], terrestrial environments are often limited by bioavailable Mo. However, the ability of microbes to extract Mo and other trace metals from minerals not

only enhances mineral weathering but also enables microbial survival and function under oligotrophic conditions.

Consideration of bioavailability of solid-phase trace metals has two broad implications. One may be improved model prediction of biological N<sub>2</sub> fixation. For example, Cleveland et al. (1999) reported a discrepancy between data-based estimate and model prediction of biological N<sub>2</sub> fixation. While there may be many reasons for such discrepancy, lack of consideration of certain limiting factors, including bioavailability of mineral-associated trace metals, may be an important one. The second implication is improved success of cultivation of environmental micro-organisms. It is well-established that only 1% of micro-organisms are culturable based on standard agar or liquid medium (Martiny, 2019). However, many micro-organisms are attached to mineral surface for energy and nutrient acquisition (Dong et al., 2022). This study demonstrated that microbes are able to extract elements from minerals for growth and functions. Therefore, a mineral-based growth medium may be more representative of natural environment and may increase the chance of success of cultivation.

### 4.3 | Implications for Mo-based N<sub>2</sub> fixation on early Earth

Although Mo-nitrogenase is the most efficient form of diazotrophy in fixing N<sub>2</sub> (Glass et al., 2009), a low level of aqueous Mo and a high level of soluble Fe in Archean oceans (Anbar, 2008) suggest that alternate nitrogenases would have been favorable. However, phylogenetic analysis (Boyd & Peters, 2013) and nitrogen isotopes (Stueken et al., 2015) suggest that Mo-based nitrogenase Nif actually emerged first and was the predominant class of enzymes responsible for biological N<sub>2</sub> fixation in the Archean oceans, long before the GOE (Mus et al., 2019). Likewise, a recent study reconstructed the evolutionary history of nitrogenase to evaluate the potential metal dependence of ancient nitrogenases and suggested that inferred ancestral sequences at the deepest nodes of the ancient nitrogenases most resemble modern Mo-nitrogenase (Garcia et al., 2020).

Our results provide a partial answer to this paradox by demonstrating that mineral-associated trace metals are bioavailable to N<sub>2</sub> fixation. The efficiency of nitrogenases using solid-form trace metals, however, is lower than those using aqueous forms. Nonetheless, the lower efficiency may be compensated by abundant Mo- and V-bearing minerals and rocks in natural environments (Greaney et al., 2018). Furthermore, the size of the biosphere on early Earth may be much smaller than today, thus the demand for fixed nitrogen may be lower. Nonetheless, the experimental conditions used in this study do not fully mimic ancient Earth. For example, the bacterium used in this study is aerobic. Furthermore, some of the Mo-binding siderophores, including azotobactin and catechol metallophores may be introduced into *A. vinelandii* genome recently (Zhang et al., 2019). While some of the minerals such as molybdenite and clay minerals were available before the GOE (Hazen et al., 2008),

others such as ferrihydrite and goethite, while present, may not be abundant until around the GOE (Hazen et al., 2008).

Future studies should focus on mineral-microbe pairs that were co-present in different geological times and specific microbial mechanisms responsible for trace metal uptake. While the mechanisms of metal uptake and the rates of N<sub>2</sub> fixation may be different with different pairs of minerals and microbes, the results of this study are significant because we demonstrate that mineral-associated trace metals can be bioavailable to essential biological functions.

## 5 | CONCLUSIONS

Nitrogen fixation by *A. vinelandii* was observed in the presence of mineral-associated trace metal cofactors but with lower rates. Possible mechanisms for such metal uptake from minerals are likely through secretion of siderophores as a result of physical attachment to mineral surface.

### ACKNOWLEDGMENTS

This study was supported by a grant from National Science Foundation (EAR-1937423). We also thank Dr. Alfredo Huerta and the Department of Biology at Miami University, Ohio and Dr. Sunjeong Park at Ohio State University, Ohio. We are grateful to subject editor Jennifer Glass and three anonymous reviewers whose comments improved the quality of the manuscript.

### CONFLICT OF INTEREST STATEMENT

The authors declare no competing interests.

### DATA AVAILABILITY STATEMENT

The authors declare that all data supporting the findings of this study are available within the paper and in the [Supporting Information](#) files.

### ORCID

Hailiang Dong  <https://orcid.org/0000-0002-7468-1350>

Yizhi Sheng  <https://orcid.org/0000-0001-7285-4695>

### REFERENCES

- Ahmed, E., & Holmstrom, S. J. M. (2015). Microbe-mineral interactions: The impact of surface attachment on mineral weathering and element selectivity by microorganisms. *Chemical Geology*, 403, 13–23.
- Amonette, J. E., & Templeton, J. C. (1998). Improvements to the quantitative assay of nonrefractory minerals for Fe(II) and total Fe using 1,10-phenanthroline. *Clays and Clay Minerals*, 46(1), 51–62. <https://doi.org/10.1346/CCMN.1998.0460106>
- Anbar, A. D. (2008). Oceans, elements and evolution. *Science*, 322, 1481–1483. <https://doi.org/10.1126/science.1163100>
- Anbar, A. D., & Knoll, A. H. (2002). Proterozoic Ocean chemistry and evolution: A bioinorganic bridge? *Science*, 297, 1137–1142. <https://doi.org/10.1126/science.1069651>
- Angerer, T., & Hagemann, S. G. (2010). The BIF-hosted high-grade iron ore deposits in the Archean Koolyanobbing Greenstone Belt, Western Australia: Structural control on synorogenic-and

- weathering-related magnetite-, hematite-, and goethite-rich iron ore. *Economic Geology*, 105, 917–945. <https://doi.org/10.2113/gsecongeo.105.5.917>
- Baars, O., Zhang, X., Morel, F. M. M., & Seyedsayamdost, M. R. (2016). The siderophore metabolome of *Azotobacter vinelandii*. *Applied and Environmental Microbiology*, 82, 27–39. <https://doi.org/10.1128/AEM.03160-15>
- Bellenger, J. P., Wichard, T., Xu, Y., & Kraepiel, A. M. (2011). Essential metals for nitrogen fixation in a free-living N<sub>2</sub>-fixing bacterium: Chelation, homeostasis and high use efficiency. *Environmental Microbiology*, 13, 1395–1411.
- Bellenger, J. P., Xu, Y., Zhang, X., Morel, F. M. M., & Kraepiel, A. M. L. (2014). Possible contribution of alternative nitrogenases to nitrogen fixation by symbiotic N<sub>2</sub>-fixing bacteria in soils. *Soil Biology & Biochemistry*, 69, 413–420. <https://doi.org/10.1016/j.soilbio.2013.11.015>
- Bernhard, A. (2010). The nitrogen cycle: Processes, players, and human impact. *Nature Education Knowledge*, 3, 25.
- Bhattacharyya, K. G., & Gupta, S. S. (2008). Kaolinite and montmorillonite as adsorbents for Fe(III), Co(II) and Ni(II) in aqueous medium. *Applied Clay Science*, 41, 1–9. <https://doi.org/10.1016/j.clay.2007.09.005>
- Bishop, P. E., Jarlenski, D. M., & Hetherington, D. R. (1982). Expression of an alternative nitrogen fixation system in *Azotobacter vinelandii*. *Journal of Bacteriology*, 150, 1244–1251. <https://doi.org/10.1128/jb.150.3.1244-1251.1982>
- Boyd, E. S., & Peters, J. W. (2013). New insights into the evolutionary history of biological nitrogen fixation. *Frontiers in Microbiology*, 4, 201. <https://doi.org/10.3389/fmicb.2013.00201>
- Chi Fru, E., Gray, N. D., McCann, C., Baptista, J. C., Christgen, B., Talbot, H. M., El Ghazouani, A., Dennison, C., & Graham, D. W. (2011). Effects of copper mineralogy and methanobactin on cell growth and sMMO activity in *Methylosinus trichosporium* OB3b. *Biogeosciences Discussion*, 8, 2851–2874. <https://doi.org/10.5194/bgd-8-2887-2011>
- Cleveland, C. C., Townsend, A. R., Schimel, D. S., Fisher, H., Howarth, R. W., Hedin, L. O., Perakis, S., Latty, E. F., Von Fischer, J. C., Elseroad, A., & Wasson, M. F. (1999). Global patterns of terrestrial biological nitrogen (N<sub>2</sub>) fixation in natural ecosystems. *Global Biogeochemical Cycles*, 13(2), 623–645. <https://doi.org/10.1029/1999GB900014>
- Collier, R. W. (1985). Molybdenum in the Northeast Pacific Ocean. *Limnology and Oceanography*, 30(6), 1351–1354.
- Dilworth, M. J. (1966). Acetylene reduction by nitrogen-fixing preparations from *Clostridium pasteurianum*. *Biochimica et Biophysica Acta*, 127, 285–294. [https://doi.org/10.1016/0304-4165\(66\)90383-7](https://doi.org/10.1016/0304-4165(66)90383-7)
- Dong, H., Huang, L., Zhao, L., Zeng, Q., Liu, X., Sheng, Y., Shi, L., Wu, G., Jiang, H., Li, F., Zhang, L., Guo, D., Li, G., Hou, W., & Chen, H. (2022). A critical review of mineral-microbe interaction and coevolution: Mechanisms and applications. *National Science Review*, 9, nwac128. <https://doi.org/10.1093/nsr/nwac128>
- Dong, H., Kostka, J. E., & Kim, J. (2003). Microscopic evidence for microbial dissolution of smectite. *Clays and Clay Minerals*, 51, 502–512. <https://doi.org/10.1346/000986003322584749>
- Dos Santos, P. C., Dean, D. R., Hu, Y., & Ribbe, M. W. (2004). Formation and insertion of the nitrogenase iron–molybdenum cofactor. *Chemical Reviews*, 104, 1159–1174. <https://doi.org/10.1021/cr020608l>
- Duhme, A. K., Hider, R. C., Naldrett, M. J., & Pau, R. N. (1998). The stability of the molybdenum-azotochelin complex and its effect on siderophore production in *Azotobacter vinelandii*. *Journal of Biological Inorganic Chemistry*, 3, 520–526.
- Dupont, C. L., Butcher, A., Valas, R. E., Bourne, P. E., & Caetano-Anollés, G. (2010). History of biological metal utilization inferred through phylogenomic analysis of protein structures. *Proceedings of the National Academy of Sciences of the United States of America*, 107, 10567–10572. <https://doi.org/10.1073/pnas.0912491107>
- Eady, R. R. (1996). Structure–function relationships of alternative nitrogenases. *Chemical Reviews*, 96, 3013–3030. <https://doi.org/10.1021/cr950057h>
- Garcia, A. K., McShea, H., Kolaczowski, B., & Kaçar, B. (2020). Reconstructing the evolutionary history of nitrogenases: Evidence for ancestral molybdenum-cofactor utilization. *Geobiology*, 18(3), 394–411. <https://doi.org/10.1111/gbi.12381>
- Glass, J. B., Wolfe-Simon, F., & Anbar, A. D. (2009). Coevolution of metal availability and nitrogen assimilation in cyanobacteria and algae. *Geobiology*, 7, 100–123. <https://doi.org/10.1111/j.1472-4669.2009.00190.x>
- Goldberg, S., Forster, H. S., & Godfrey, C. L. (1996). Molybdenum adsorption on oxides, clay minerals, and soils. *Soil Science Society of America Journal*, 60, 425–432. <https://doi.org/10.2136/sssaj1996.03615995006000020013x>
- Greaney, A. T., Rudnick, R. L., Gaschnig, R. M., Whalen, J. B., Luais, B., & Clemens, J. D. (2018). Geochemistry of molybdenum in the continental crust. *Geochimica et Cosmochimica Acta*, 238, 36–54. <https://doi.org/10.1016/j.gca.2018.06.039>
- Gustafsson, J. P. (2003). Modelling molybdate and tungstate adsorption to ferrihydrite. *Chemical Geology*, 200, 105–115. <https://doi.org/10.1016/s0009-6>
- Hausrath, E. M., Liermann, L. J., House, C. H., Ferry, J. G., & Brantley, S. L. (2007). The effect of methanogen growth on mineral substrates: Will Ni markers of methanogen-based communities be detectable in the rock record? *Geobiology*, 5(1), 49–61. <https://doi.org/10.1111/j.1472-4669.2007.00095.x>
- Hazen, R. M., Liu, X.-M., Downs, R. T., Golden, J., Pires, A. J., Grew, E. S., Hystad, G., Estrada, C., & Sverjensky, D. A. (2014). Mineral evolution: Episodic metallogenesis, the supercontinent cycle, and the coevolving geosphere and biosphere. *Society of Economic Geologist*, 18, 1–15.
- Hazen, R. M., Papineau, D., Bleeker, W., Downs, R. T., Ferry, J. M., McCoy, T. J., Sverjensky, D. A., & Yang, H. (2008). Mineral evolution. *American Mineralogist*, 93, 1693–1720. <https://doi.org/10.2138/am.2008.2955>
- Jelen, B. I., Giovannelli, D., & Falkowski, P. G. (2016). The role of microbial electron transfer in the coevolution of the biosphere and geosphere. *Annual Review of Microbiology*, 70, 45–62. <https://doi.org/10.1146/annurev-micro-102215-095521>
- Johnson, A. C., Ostrander, C. M., Romaniello, S. J., Reinhard, C. T., Greaney, A. T., Lyons, T. W., & Anbar, A. D. (2021). Reconciling evidence of oxidative weathering and atmospheric anoxia on Archaean Earth. *Science Advances*, 7, eabj0108.
- Knapp, C. W., Fowle, D. A., Kulczycki, E., Roberts, J. A., & Graham, D. W. (2007). Methane monooxygenase gene expression mediated by methanobactin in the presence of mineral copper sources. *Proceedings of the National Academy of Sciences of the United States of America*, 104, 12040–12045. <https://doi.org/10.1073/pnas.0702879104>
- Konhauser, K. O., Newman, D. K., & Kappler, A. (2005). The potential significance of microbial Fe(III) reduction during deposition of Precambrian banded iron formations. *Geobiology*, 3, 167–177. <https://doi.org/10.1111/j.1472-4669.2005.00055.x>
- Kraemer, D., Frei, R., Viehmann, S., & Bau, M. (2019). Mobilization and isotope fractionation of chromium during water-rock interaction in presence of siderophores. *Applied Geochemistry*, 102, 44–54. <https://doi.org/10.1016/j.apgeochem.2019.01.007>
- Kulczycki, E., Fowle, D. A., Kenward, P. A., Leslie, K., Graham, D. W., & Roberts, J. A. (2011). Stimulation of methanotroph activity by Cu-substituted borosilicate glass. *Geomicrobiology Journal*, 28(1), 1–10. <https://doi.org/10.1080/01490451003614971>
- Liermann, L. J., Guynn, R. L., Anbar, A., & Brantley, S. L. (2005). Production of a molybdophore during metal-targeted dissolution of silicates by soil bacteria. *Chemical Geology*, 220, 285–302. <https://doi.org/10.1016/j.chemgeo.2005.04.013>

- Martiny, A. C. (2019). High proportions of bacteria are culturable across major biomes. *ISME Journal*, 13, 2125–2128. <https://doi.org/10.1038/s41396-019-0410-3>
- McRose, D. L., Baars, O., Morel, F. M. M., & Kraepiel, A. M. L. (2017). Siderophore production in *Azotobacter vinelandii* in response to Fe-, Mo- and V-limitation. *Environmental Microbiology*, 19, 3595–3605. <https://doi.org/10.1111/1462-2920.13857>
- Moore, E. K., Jelen, B. I., Giovannelli, D., Raanan, H., & Falkowski, P. G. (2017). Metal availability and the expanding network of microbial metabolisms in the Archaean eon. *Nature Geoscience*, 10(9), 629–636. <https://doi.org/10.1038/ngeo3006>
- Mukhtar, H., Bashir, H., Nawaz, A., & Haq, I. (2018). Optimization of growth conditions for *Azotobacter* species and their use as biofertilizer. *Journal of Bacteriology & Mycology*, 6(5), 274–278. <https://doi.org/10.15406/jbmoa.2018.06.00217>
- Mus, F., Colman, D. R., Peters, J. W., & Boyd, E. S. (2019). Geobiological feedbacks, oxygen, and the evolution of nitrogenase. *Free Radical Biology and Medicine*, 140, 250–259. <https://doi.org/10.1016/j.freeradbiomed.2019.01.050>
- Mus, F., Tseng, A., Dixon, R., & Peters, J. W. (2017). Diazotrophic growth allows *Azotobacter vinelandii* to overcome the deleterious effects of a glnE deletion. *Applied and Environmental Microbiology*, 83(13), e00808-17. <https://doi.org/10.1128/AEM.00808-17>
- Parsons, C., Stüeken, E. E., Rosen, C. J., Mateos, K., & Anderson, R. E. (2021). Radiation of nitrogen-metabolizing enzymes across the tree of life tracks environmental transitions in Earth history. *Geobiology*, 19(1), 18–34. <https://doi.org/10.1111/gbi.12419>
- Peacock, C. L., & Sherman, D. M. (2004). Vanadium (V) adsorption onto goethite ( $\alpha$ -FeOOH) at pH 1.5 to 12: A surface complexation model based on ab initio molecular geometries and EXAFS spectroscopy. *Geochimica et Cosmochimica Acta*, 68, 1723–1733. <https://doi.org/10.1016/j.gca.2003.10.018>
- Rai, V., Fisher, N., Duckworth, O. W., & Baars, O. (2020). Extraction and detection of structurally diverse siderophores in soil. *Frontiers in Microbiology*, 11, 581508. <https://doi.org/10.3389/fmicb.2020.581508>
- Robson, R. L., Eady, R. R., Richardson, T. H., Miller, R. W., Hawkins, M., & Postgate, J. R. (1986). The alternative nitrogenase of nitrogenase of *Azotobacter chroococcum* is a vanadium enzyme. *Nature*, 322, 388–390. <https://doi.org/10.1038/322388a0>
- Schwertmann, U., & Cornell, R. M. (2007). Goethite. In U. Schwertmann & R. M. Cornell (Eds.), *Iron oxides in the laboratory: Preparation and characterization* (2nd ed., pp. 67–92). Wiley VCH Verlag.
- Scott, C., Lyons, T. W., Bekker, A., Shen, Y., Poulton, S. W., Chu, X., & Anbar, A. D. (2008). Tracing the stepwise oxygenation of the Proterozoic Ocean. *Nature*, 452, 456–459. <https://doi.org/10.1038/nature06811>
- Srivastava, S., Briggs, B. R., & Dong, H. (2018). Abundance and taxonomic affiliation of molybdenum transport and utilization genes in Tengchong hot springs, China. *Environmental Microbiology*, 20, 2397–2409. <https://doi.org/10.1111/1462-2920.14250>
- Stueken, E. E., Buick, R., Guy, B. M., & Koehler, M. C. (2015). Isotopic evidence for biological nitrogen fixation by molybdenum-nitrogenase from 3.2 Gyr. *Nature*, 520, 666–669. <https://doi.org/10.1038/nature14180>
- Ward, B. (2012). The global nitrogen cycle. In A. H. Knoll, D. E. Canfield, & K. Konhauser (Eds.), *Fundamentals of geobiology* (pp. 36–48). John Wiley & Sons.
- Warren, M. J., Lin, X., Gaby, J. C., Kretz, C. B., Kolton, M., Morton, P. L., Pett-ridge, J., Weston, D. J., Schadt, C. W., Kostka, J. E., & Glass, B. (2017). Molybdenum-based diazotrophy in a sphagnum peatland in northern Minnesota. *Applied and Environmental Microbiology*, 83, 1–14. <https://doi.org/10.1128/AEM.01174-17>
- Wichard, T., Bellenger, J. P., Morel, F. M. M., & Kraepiel, A. M. L. (2009). Role of the siderophore azotobactin in the bacterial acquisition of nitrogenase metal cofactors. *Environmental Science & Technology*, 43, 7218–7224. <https://doi.org/10.1021/es8037214>
- Zhang, X., Baars, O., & Morel, F. M. M. (2019). Genetic, structural, and functional diversity of low and high-affinity siderophores in strains of nitrogen fixing *Azotobacter chroococcum*. *Metallomics*, 11, 201–212.
- Zhang, Y., & Gladyshev, V. N. (2011). Comparative genomics of trace element dependence in biology. *Journal of Biological Chemistry*, 286, 23623–23629. <https://doi.org/10.1074/jbc.R110.172833>

#### SUPPORTING INFORMATION

Additional supporting information can be found online in the Supporting Information section at the end of this article.

**How to cite this article:** Srivastava, S., Dong, H., Baars, O., & Sheng, Y. (2023). Bioavailability of mineral-associated trace metals as cofactors for nitrogen fixation by *Azotobacter vinelandii*. *Geobiology*, 00, 1–13. <https://doi.org/10.1111/gbi.12552>